Available online at www.sciencedirect.com

ScienceDirect

Inorganica Chimica Acta 360 (2007) 2128–2138

Inorganica Chimica Acta

www.elsevier.com/locate/ica

Synthesis, characterization and catalytic evaluation in the Heck coupling reactions of S–P–S pincer complexes of the type [Pd{PhP(C_6H_4-2-S)$_2$}(PAr$_3$)]

Valente Gómez-Benítez, Simón Hernández-Ortega, Rubén A. Toscano, David Morales-Morales *

Instituto de Química, Universidad Nacional Autónoma de México, Cd. Universitaria, Circuito Exterior, Coyoacán 04510 México DF, Mexico

Received 2 August 2006; received in revised form 18 October 2006; accepted 29 October 2006
Available online 9 November 2006

Abstract

A series of palladium complexes of the type [Pd(*ph*PS$_2$)(PAr$_3$)] (*ph*PS$_2$) = [PhP(C_6H_4-2-S)$_2$]$^{2-}$ have been synthesized in good yields and their crystal structures determined. Heck coupling reactions were carried out using the [Pd(*ph*PS$_2$)(PPh$_3$)] (**1**), [Pd(*ph*PS$_2$){P(C_6H_4-4-Cl)$_3$}] (**2**), [Pd(*ph*PS$_2$){P(C_6H_4-4-F)$_3$}] (**3**), [Pd(*ph*PS$_2$){P(C_6H_4-4-CF$_3$)$_3$}] (**4**), [Pd(*ph*PS$_2$){P(C_6H_4-4-Me)$_3$}] (**5**) and [Pd(*ph*PS$_2$){P(C_6H_4-4-OMe)$_3$}] (**6**) complexes as catalyst precursors in order to examine the potential effect of the *para*-substituted triarylphosphines in the reaction of bromobenzene and styrene.

Keywords: S–P–S pincer complexes; Hemilability; Heck reaction; C–C coupling reactions; Triarylphosphines; Palladium complexes; Crystal structures; Catalysis

1. Introduction

The importance that transition metal catalyzed reactions have acquired in modern organic chemistry [1] has been so vast that some transformations are simply unconceivable without the use of transition metal catalysts. This, being particularly true in the case of cross-coupling reactions [2]. Among them, palladium catalyzed C–C coupling reactions have been recognized as power tools in multiple organic transformations, from these the Heck reaction has been denominated as an angular stone in modern organic synthesis [3]. This reaction consists in the coupling of a halo compound with a double bond. The multiple applications of this reaction have been clearly identified and efforts aimed to explore its potential use at the industrial level [4] are a continuous research topic both at the academic and industrial level. These facts have led both inorganic and organic chemists around the world to the search of cheap, easy to synthesize, highly active and stable catalysts. In this sense, in recent years, several groups have been involved in the design of ligands able to afford robust catalysts, capable of withstand a variety of reaction conditions and oxidant atmospheres, that would favor Heck couplings in an efficient manner with cheap reagent grade starting materials. From all the compounds employed so far, it seems that polydentated ligands incorporating both thiolate and tertiary phosphine donor ligands may offer an interesting option to carry out this process [5]. Moreover, the presence of these ligands in the coordination sphere of transition metal complexes may render interesting behaviors in solution as these ligands can be capable of full or partial de-ligation (hemilability) [6], being able to provide important extra coordination sites for incoming substrates during a catalytic process [6]. Thus, given our continuous interest in the design and synthesis of transition metal complexes for potential application in industrial relevant

---

* Corresponding author. Tel.: +52 55 56224514; fax: +52 55 56162217.
E-mail address: damor@servidor.unam.mx (D. Morales-Morales).

0020-1693/$ - see front matter © 2006 Elsevier B.V. All rights reserved.
doi:10.1016/j.ica.2006.10.029

catalytic transformations [7], we would like to report here the use of the pincer type S–P–S proligand [*ph*PS_2H_2] and *p*-substituted triaryl phosphines as substituents for the fine tuning of the electronics in the synthesis of a series of Pd(II) complexes of the type [Pd(*ph*PS_2)(PAr_3)]. The identification of the electronic effects of the different *p*-substituted triarylphosphines over the properties and reactivity of these species in the palladium catalyzed Heck reaction of bromobenzene with olefins will be discussed.

2. Experimental

2.1. Material and methods

Unless stated otherwise, all reactions were carried out under an atmosphere of dinitrogen using conventional Schlenk glassware, solvents were dried using established procedures and distilled under dinitrogen immediately prior to use. The IR spectra were recorded on a Nicolet-Magna 750 FT-IR spectrometer as Nujol mulls. The ^1H NMR spectra were recorded on a JEOL GX300 spectrometer. Chemical shifts are reported in ppm downfield of TMS using the solvent ($CDCl_3$, δ 7.27) as the internal standard. ^{31}P NMR spectra were recorded with complete proton decoupling and are reported in ppm using 85% H_3PO_4 as the external standard. Elemental analyses were determined on a Perkin Elmer 240. Positive-ion FAB mass spectra were recorded on a JEOL JMS-SX102A mass spectrometer operated at an accelerating voltage of 10 kV. The samples were desorbed from a nitrobenzyl alcohol (NOBA) matrix using 3 keV xenon atoms. Mass measurements in FAB are performed at a resolution of 3000 using magnetic field scans and the matrix ions as the reference material or, alternatively, by electric field scans with the sample peak bracketed by two (polyethylene glycol or cesium iodide) reference ions. The $K_2[PdCl_4]$ was obtained from Aldrich Chemical Co. and the phosphines $P(C_6H_5)_3$, $P(C_6H_4\text{-}4\text{-}Cl)_3$, $P(C_6H_4\text{-}4\text{-}F)_3$, $P(C_6H_4\text{-}4\text{-}CF_3)_3$, $P(C_6H_4\text{-}4\text{-}Me)_3$ and $P(C_6H_4\text{-}4\text{-}OMe)_3$ were purchased from STREM Chemicals, Inc. All compounds were used as received without further purification. The proligand *ph*PS_2H_2 [8] and the starting materials *trans*-[$PdCl_2(PAr_3)_2$] [9] were prepared according to published procedures.

2.2. General procedure for the synthesis of complexes [Pd(phPS$_2$)(PAr$_3$)]

Complexes **1**–**6** were synthesized by using the same experimental procedure. Thus, as a representative example, the synthesis of [Pd(*ph*PS_2)(PPh_3)] (**1**) is described [10].

2.2.1. Synthesis of bis[(2-phenylthiolato)phenylphosphino-S,S′,P]-triphenylphosphine-palladium(II), [Pd(phPS$_2$)(PPh$_3$)] (1)

To a solution of *trans*-[$PdCl_2(PPh_3)_2$] (428 mg, 0.613 mmol) in CH_2Cl_2 (10 cm^3) a solution (10 cm^3) of 1 equiv. of the phosphino-dithiol *ph*PS_2H_2 (200 mg, 0.613 mmol) and NEt_3 (0.116 mg, 1.227 mmol) was added. The solution was stirred for 24 h. Following the reaction time the solution was filtered off and the volume reduced in vacuum to obtain a reddish-brown residue that was recrystallized from a double layer solvent system of CH_2Cl_2/MeOH. Yield 372 mg (87%). Mp 253–256 °C. RMN $^{31}P\{^1H\}$ (121 MHz, $CDCl_3$) δ 85.33 (d, $J^2_{PP} =$ 405.6 Hz, 1P), 22.76 (d, $J^2_{PP} = 405.6$ Hz, 1P). MS–FAB$^+$ $[M]^+ = 692$ (53%), $[M\text{–}PPh_3]^+ = 430$ (25%), [M–Pd*ph*$PS_2]^+ = 263$ (100%) *m*/*z*. *Anal.* Calc. for $C_{36}H_{28}P_2PdS_2$ (Mw = 693.11): C, 62.38; H, 4.07. Found: C, 61.13; H, 3.98%.

2.2.2. Synthesis of bis[(2-phenylthiolato)phenylphosphino-S,S′,P]-tris(4-chlorophenyl)phosphine-palladium(II), [Pd(phPS$_2$){P(C$_6$H$_4$-4-Cl)$_3$}] (2)

trans-[$PdCl_2\{P(C_6H_4\text{-}4\text{-}Cl)_3\}_2$] (557 mg, 0.613 mmol). Yield 432 mg (81%). Mp 240–242 °C. RMN $^{31}P\{^1H\}$ (121 MHz, $CDCl_3$) δ 86.04 (d, $J^2_{PP} = 408$ Hz, 1P), 21.29 (d, $J^2_{PP} = 408$ Hz, 1P). MS–FAB$^+$ $[M]^+ = 795$ (18%), $[M\text{–}P(C_6H_4\text{-}4\text{-}Cl)_3]^+ = 430$ (16%), [M–Pd*ph*$PS_2]^+ = 365$ (8%) *m*/*z*. *Anal.* Calc. for $C_{36}H_{25}Cl_3P_2PdS_2$ (Mw = 796.44): C, 54.29; H, 3.16. Found: C, 53.21; H, 3.09%.

2.2.3. Synthesis of bis[(2-phenylthiolato)phenylphosphino-S,S′,P]-tris(4-fluorophenyl)phosphine-palladium(II), [Pd(phPS$_2$){P(C$_6$H$_4$-4-F)$_3$}] (3)

trans-[$PdCl_2\{P(C_6H_4\text{-}4\text{-}F)_3\}_2$] (497 mg, 0.613 mmol). Yield 417 mg (83%). Mp 242 °C. RMN $^{31}P\{^1H\}$ (121 MHz, $CDCl_3$) δ 85.74 (d, $J^2_{PP} = 408$ Hz, 1P), 20.58 (d, $J^2_{PP} = 408$ Hz, 1P). MS–FAB$^+$ $[M]^+ = 746$ (57%), $[M\text{–}P(C_6H_4\text{-}4\text{-}F)_3]^+ = 430$ (34%), [M–Pd*ph*$PS_2]^+ = 317$ (44%) *m*/*z*. *Anal.* Calc. for $C_{36}H_{25}F_3P_2PdS_2$ (Mw = 747.08): C, 57.88; H, 3.37. Found: C, 56.70; H, 3.31%.

2.2.4. Synthesis of bis[(2-phenylthiolato)phenylphosphino-S,S′,P]-tris(4-trifluoromethylphenyl)phosphine-palladium(II), [Pd(phPS$_2$){P(C$_6$H$_4$-4-CF$_3$)$_3$}] (4)

trans-[$PdCl_2\{P(C_6H_4\text{-}4\text{-}CF_3)_3\}_2$] (681 mg, 0.613 mmol). Yield 494 mg (83%). Mp 230 °C $^{31}P\{^1H\}$ (121 MHz, $CDCl_3$) δ 86.78 (d, $J^2_{PP} = 403$ Hz, 1P), 23.12 (d, $J^2_{PP} =$ 403 Hz, 1P). MS–FAB$^+$ $[M]^+ = 896$ (37%), [M–Pd*ph*$PS_2]^+ = 466$ (100%), $[M\text{–}P(C_6H_4\text{-}4\text{-}CF_3)_3]^+ = 430$ (44%) *m*/*z*. *Anal.* Calc. for $C_{39}H_{25}F_9P_2PdS_2$ (Mw = 897.1): C, 52.21; H, 2.81. Found: C, 51.68; H, 2.78%.

2.2.5. Synthesis of bis[(2-phenylthiolato)phenylphosphino-S,S′,P]-tris(4-methylphenyl)phosphine-palladium(II), [Pd(phPS$_2$){P(C$_6$H$_4$-4-Me)$_3$}] (5)

trans-[$PdCl_2\{P(C_6H_4\text{-}4\text{-}Me)_3\}_2$] (482 mg, 0.613 mmol). Yield 446 mg (90%). Mp 221 °C. RMN $^{31}P\{^1H\}$ (121 MHz, $CDCl_3$) δ 84.89 (d, $J^2_{PP} = 408$ Hz, 1P), 20.86 (d, $J^2_{PP} = 408$ Hz, 1P). MS–FAB$^+$ $[M]^+ = 734$ (18%), $[M\text{–}P(C_6H_4\text{-}4\text{-}Me)_3]^+ = 430$ (7%), [M–Pd*ph*$PS_2]^+ = 305$ (100%) *m*/*z*. *Anal.* Calc. for $C_{39}H_{34}P_2PdS_2$ (Mw = 735.18): C, 63.71; H, 4.66. Found: C, 62.58; H, 4.58%.

2.2.6. Synthesis of bis[(2-phenylthiolato)phenylphosphino-S,S′,P]-tris(4-methoxyphenyl)phosphine-palladium(II), [Pd(phPS$_2$){P(C$_6$H$_4$-4-OMe)$_3$}] (**6**)

trans-[PdCl$_2${P(C$_6$H$_4$-4-OMe}$_3$)$_2$] (540 mg, 0.613 mmol). Yield 367 mg (70%). Mp 218–220 °C. RMN ^{31}P{^{1}H} (121 MHz, CDCl$_3$) δ 84.59 (d, $J^2_{\mathrm{PP}} = 419$ Hz, 1P), 19.13 (d, $J^2_{\mathrm{PP}} = 419$ Hz, 1P). MS–FAB$^+$ [M]$^+$ = 781 (15%), [M–P-(C$_6$H$_4$-4-OMe)$_3$]$^+$ = 430 (4%), [M–Pd*ph*PS$_2$]$^+$ = 353 (27%) *m/z*. *Anal.* Calc. for $C_{39}H_{34}O_3P_2PdS_2$ (Mw = 783.18): C, 59.81; H, 4.38. Found: C, 60.41; H, 4.40%.

2.3. General procedure for the catalytic reactions

A DMF solution (5 mL) of 2.5 mmol of bromobenzene, 3.2 mmol of styrene, and the prescribed amount of catalyst (4.33×10^{-3} mmol) was introduced into a Schlenk tube in open air. The tube was charged with a magnetic stir bar and an excess of Cs_2CO_3 (3.77 mmol) as base, sealed, and fully immersed in a 160 °C silicon oil bath. After the prescribed reaction time (4 h), the mixture was cooled to room temperature and the organic phase was analyzed by gas chromatography (GC–MS) coupled to a selective mass detector.

2.4. Data collection and refinement for [Pd(phPS$_2$){P(C$_6$H$_4$-4-Cl)$_3$}] (**2**), [Pd(phPS$_2$){P(C$_6$H$_4$-4-F)$_3$}] (**3**), [Pd(phPS$_2$){P(C$_6$H$_4$-4-Me)$_3$}] (**5**), [Pd(phPS$_2$){P(C$_6$H$_4$-4-OMe)$_3$}] (**6**)

Crystalline orange-red prisms for **2**, **3**, **5** and **6** were grown independently by a slow evaporation of CH_2Cl_2/MeOH solvent systems, and mounted on glass fibers. In all cases, the X-ray intensity data were measured at 293 or 291 K on a Bruker SMART APEX CCD-based X-ray diffractometer system equipped with a Mo-target X-ray tube ($\lambda = 0.71073$ Å). The detector was placed at a distance of 4.837 cm from the crystals in all cases. A total of 1800 frames were collected with a scan width of 0.3 in ω and an exposure time of 10 s/frame. The frames were integrated with the Bruker SAINT software package [11] using a narrow-frame integration algorithm. The integration of the data was done using a monoclinic unit cell for **3** and **6**, triclinic for **2** and orthorhombic for **5**, to yield a total of 40314, 6015, 27143 and 28099 reflections for **2**, **3**, **5** and **6**, respectively to a maximum 2θ angle of 50.00 (0.93 Å resolution), of which 11920 (**2**), 5674 (**3**), 6038 (**5**) and 6157 (**6**) were independent. Analysis of the

Table 1
Summary of crystal structure data for [Pd(*ph*PS$_2$)(PAr$_3$)] Ar = C$_6$H$_4$-4-Cl (**2**), C$_6$H$_4$-4-F (**3**), C$_6$H$_4$-4-Me (**5**), C$_6$H$_4$-4-OMe (**6**)

Compound	**2**	**3**	**5**	**6**
Empirical formula	$C_{36}H_{25}Cl_3P_2PdS_2$	$C_{36}H_{25}F_3P_2PdS_2$	$C_{39}H_{34}P_2PdS_2$	$C_{39}H_{34}O_3P_2PdS_2$
Formula weight	796.37	747.02	735.12	783.12
Temperature (K)	293(2)	291(2)	291(2)	293(2)
Crystal system	triclinic	monoclinic	orthorhombic	monoclinic
Space group	$P\bar{1}$	$P2_1/n$	$Pna2_1$	$P2_1/n$
a (Å)	13.288(1)	10.2551(14)	21.0875(12)	14.847(1)
b (Å)	13.294(1)	15.4527(18)	10.2671(6)	12.829(1)
c (Å)	19.817(1)	20.9365(15)	15.9009(9)	19.403(1)
α (°)	105.283(1)	90	90	90
β (°)	93.742(1)	103.801(7)	90	109.392(1)
γ (°)	91.615(1)	90	90	90
Volume (Å^3)	3365.9(4)	3222.0(6)	3442.7(3)	3486.1(4)
Z	4	4	4	4
D_{calc} (g/cm^3)	1.572	1.540	1.418	1.492
Absorption coefficient (mm^{-1})	1.035	0.848	0.780	0.782
F(000)	1600	1504	1504	1600
Crystal size (mm)	0.39 × 0.224 × 0.054	0.40 × 0.28 × 0.20	0.26 × 0.20 × 0.04	0.484 × 0.168 × 0.056
θ Range for data collection (°)	1.66–25.07	1.66–25.00	1.93–24.99	1.94–25.02
Index ranges	$-15 \leqslant h \leqslant 15$, $-15 \leqslant k \leqslant 15$, $-22 \leqslant l \leqslant 23$	$0 \leqslant h \leqslant 12$, $0 \leqslant k \leqslant 18$, $-24 \leqslant l \leqslant 24$	$-25 \leqslant h \leqslant 25$, $-12 \leqslant k \leqslant 12$, $-18 \leqslant l \leqslant 18$	$-17 \leqslant h \leqslant 17$, $-15 \leqslant k \leqslant 15$, $-23 \leqslant l \leqslant 23$
Reflections collected	40314	6015	27143	28099
Independent reflections	11920 [$R_{\mathrm{int}} = 0.0771$]	5674 [$R_{\mathrm{int}} = 0.0277$]	6038 [$R_{\mathrm{int}} = 0.0661$]	6157 [$R_{\mathrm{int}} = 0.0920$]
Absorption correction	analytical face indexed	none	none	analytical face indexed
Data/restraints/parameters	11920/0/793	5674/0/398	6038/1/400	6157/0/427
Final R indices [$I > 2\sigma(I)$]	$R_1 = 0.0594$, $wR_2 = 0.0682$	$R_1 = 0.0303$, $wR_2 = 0.0522$	$R_1 = 0.0464$, $wR_2 = 0.0909$	$R_1 = 0.054$, $wR_2 = 0.0608$
R indices (all data)	$R_1 = 0.1145$, $wR_2 = 0.0771$	$R_1 = 0.0503$, $wR_2 = 0.0550$	$R_1 = 0.053$, $wR_2 = 0.0940$	$R_1 = 0.1025$, $wR_2 = 0.0688$
Goodness-on-fit-on F^2	0.957	0.889	1.004	0.955

Table 2
Selected bond lengths (Å) and angles (°) for [Pd(*ph*PS$_2$){(P(C$_6$H$_4$-4-Cl)$_3$)}] (**2**), [Pd(*ph*PS$_2$){(P(C$_6$H$_4$-4-F)$_3$)}] (**3**), [Pd(*ph*PS$_2$){(P(C$_6$H$_4$-4-Me)$_3$)}] (**5**), [Pd(*ph*PS$_2$){(P(C$_6$H$_4$-4-OMe)$_3$}] (**6**)

Bond lengths (Å)

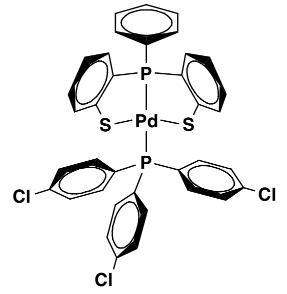

(2)

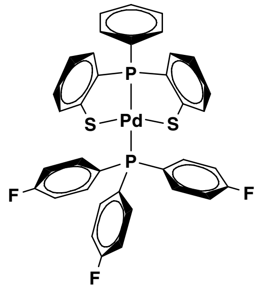

(3)

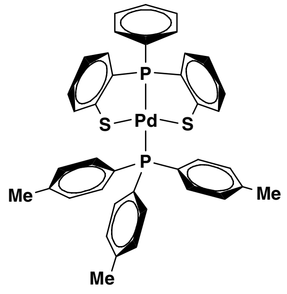

(5)

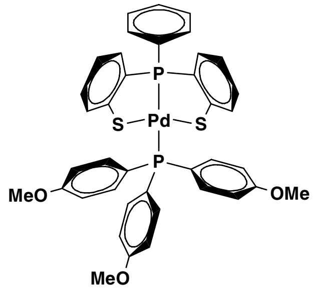

(6)

Pd(1)–P(1)	2.2286(15)	Pd(1)–P(1)	2.2274(9)	Pd(1)–P(1)	2.2254(14)	Pd(1)–P(1)	2.2225(14)
Pd(1)–S(2)	2.3085(16)	Pd(1)–S(2)	2.3110(10)	Pd(1)–S(2)	2.3041(14)	Pd(1)–S(1)	2.3171(13)
Pd(1)–S(1)	2.3106(16)	Pd(1)–S(1)	2.3370(10)	Pd(1)–S(1)	2.3342(16)	Pd(1)–S(2)	2.3190(14)
Pd(1)–P(2)	2.3443(15)	Pd(1)–P(2)	2.3598(9)	Pd(1)–P(2)	2.3690(14)	Pd(1)–P(2)	2.3660(13)
Bond angles (°)							
P(1)–Pd(1)–S(2)	86.68(6)	P(1)–Pd(1)–S(2)	86.30(4)	P(1)–Pd(1)–S(2)	86.19(5)	P(1)–Pd(1)–S(1)	85.51(5)
P(1)–Pd(1)–S(1)	85.62(6)	P(1)–Pd(1)–S(1)	84.18(3)	P(1)–Pd(1)–S(1)	84.54(6)	P(1)–Pd(1)–S(2)	85.03(5)
S(2)–Pd(1)–S(1)	161.80(6)	S(2)–Pd(1)–S(1)	165.21(4)	S(2)–Pd(1)–S(1)	162.03(7)	S(1)–Pd(1)–S(2)	164.37(5)
P(1)–Pd(1)–P(2)	178.04(7)	P(1)–Pd(1)–P(2)	173.07(3)	P(1)–Pd(1)–P(2)	176.28(6)	P(1)–Pd(1)–P(2)	175.76(5)
S(2)–Pd(1)–P(2)	94.49(6)	S(2)–Pd(1)–P(2)	92.19(4)	S(2)–Pd(1)–P(2)	94.64(5)	S(1)–Pd(1)–P(2)	98.71(5)
S(1)–Pd(1)–P(2)	93.71(6)	S(1)–Pd(1)–P(2)	98.56(3)	S(1)–Pd(1)–P(2)	95.60(5)	S(2)–Pd(1)–P(2)	90.91(5)

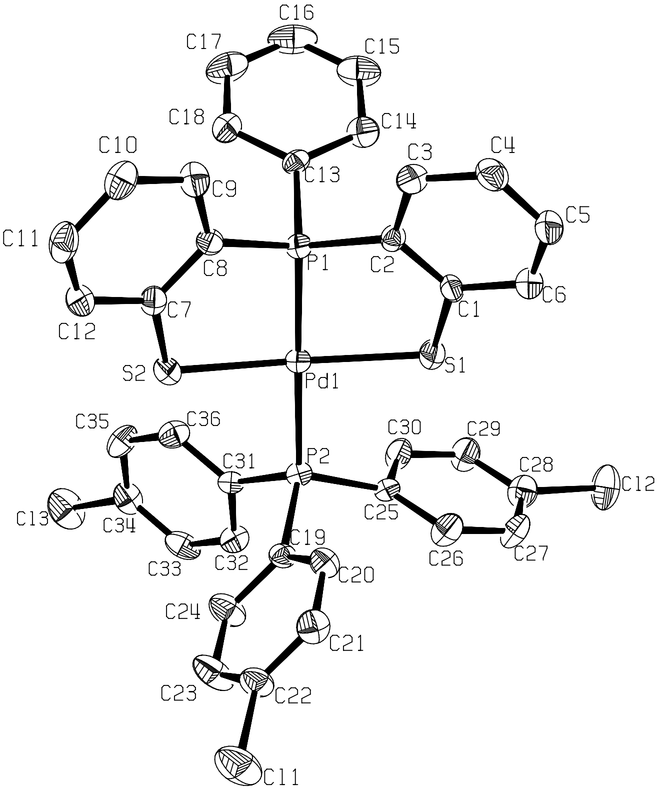

Fig. 1. An ORTEP representation of the structure of [Pd(*ph*PS$_2$){P(C$_6$H$_4$-4-Cl)$_3$}] (**2**). Displacement ellipsoids are drawn at 50% probability level showing the atom labeling scheme. Hydrogen atoms have been omitted for clarity.

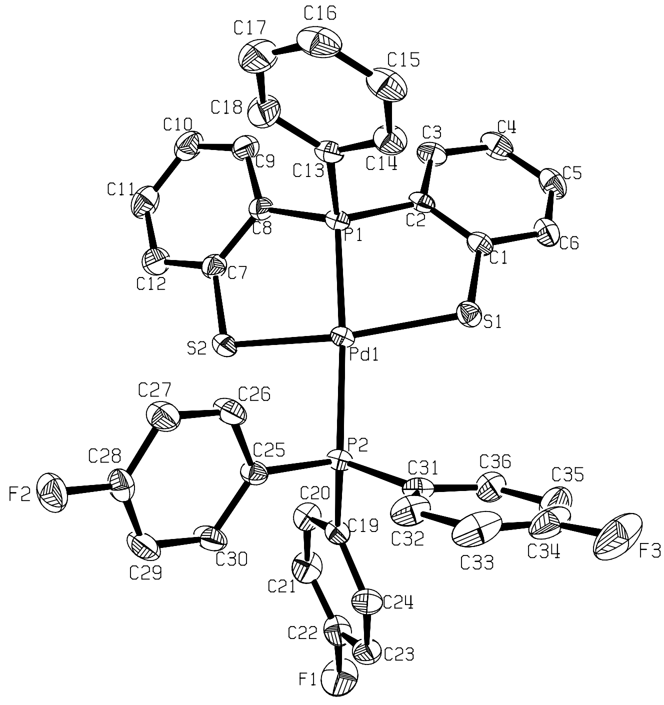

Fig. 2. An ORTEP representation of the structure of [Pd(*ph*PS$_2$){P(C$_6$H$_4$-4-F)$_3$}] (**3**). Displacement ellipsoids are drawn at 50% probability level showing the atom labeling scheme. Hydrogen atoms have been omitted for clarity.

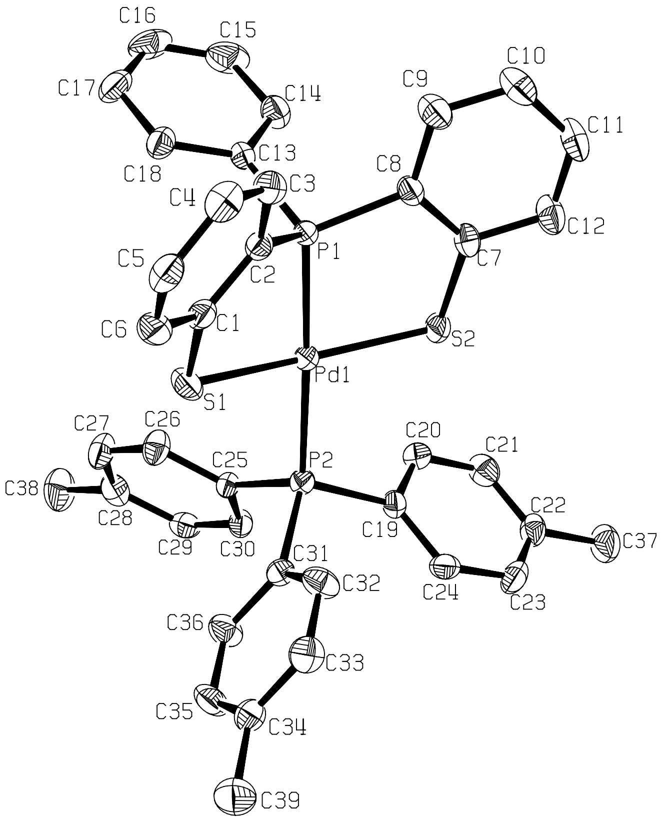

Fig. 3. An ORTEP representation of the structure of [Pd(*ph*PS_2){P(C_6H_4-4-Me)$_3$}] (**5**). Displacement ellipsoids are drawn at 50% probability level showing the atom labeling scheme. Hydrogen atoms have been omitted for clarity.

data showed in all cases negligible decays during data collections. The structures were solved by Patterson method using SHELXS-97 [12] program. The remaining atoms were located via a few cycles of least squares refinements and difference Fourier maps, using the space group $P2_1/n$ with $Z = 4$ for **3** and **6**, $P\bar{1}$ with $Z = 4$ for **2** and $Pna2_1$ with $Z = 4$ for **5**. Hydrogen atoms were input at calculated positions, and allowed to ride on the atoms to which they are attached. Thermal parameters were refined for hydrogen atoms on the phenyl groups using a $U_{eq} = 1.2$ Å to precedent atom in all cases. For all complexes, the final cycle of refinement was carried out on all non-zero data using SHELXL-97 and anisotropic thermal parameters for all non-hydrogen atoms. The details of structure determinations are given in Table 1 and selected bond lengths (Å) and angles (°) are given in Table 2. The numbering of atoms is shown in Figs. 1–4, respectively (ORTEP) [13].

3. Results and discussion

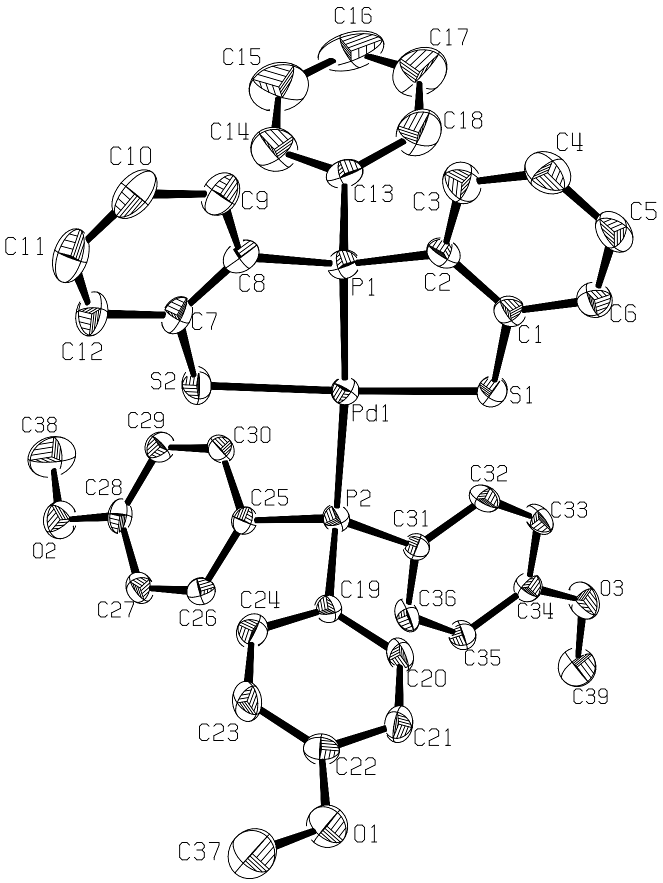

Fig. 4. An ORTEP representation of the structure of [Pd(*ph*PS_2){P(C_6H_4-4-OMe)$_3$}] (**6**). Displacement ellipsoids are drawn at 50% probability level showing the atom labeling scheme. Hydrogen atoms have been omitted for clarity.

As we have previously described for [Pd(*ph*PS_2)(PPh_3)] (**1**) [10], the synthesis of the analogous complexes [Pd(*ph*PS_2){P(C_6H_4-4-Cl)$_3$}] (**2**), [Pd(*ph*PS_2){P(C_6H_4-4-F)$_3$}] (**3**), [Pd(*ph*PS_2){P(C_6H_4-4-CF_3)$_3$}] (**4**), [Pd(*ph*PS_2){P(C_6H_4-4-Me)$_3$}] (**5**) and [Pd(*ph*PS_2){P(C_6H_4-4-OMe)$_3$}] (**6**) was carried out by reacting the corresponding palladium starting materials *trans*-[$PdCl_2(PAr_3)_2$] $PAr_3 =$ P(C_6H_4-4-Cl)$_3$, P(C_6H_4-4-F)$_3$, P(C_6H_4-4-CF_3)$_3$, P(C_6H_4-4-Me)$_3$ and P(C_6H_4-4-OMe)$_3$ with 1 equiv. of the sulfur proligand *ph*PS_2H_2 in the presence of triethylamine as base (Scheme 1).

Given the structural similarities between these complexes they also share a number of common features. Thus, in all cases the infrared spectrum does not result very informative and analyses by ^{1}H NMR techniques exhibit in all cases signals corresponding to the presence of the phenyl rings in the corresponding molecules and in the particular case of complexes **5** and **6** signals due to the CH_3 groups in the phosphino ligands at δ 2.34 and 3.80 ppm, respectively, were also observed.

The $^{31}P\{^1H\}$ NMR analysis results more interesting, showing in all cases two doublets in the spectrum, one at lower field due to the tridentated ligand *ph*$PS_2{}^{-2}$ and the other at higher field due to the PAr_3 ligands, respectively. The multiplicity of these signals in all cases is in agreement with a mutually *trans* conformation of the two phosphorus ligands [14]. The coupling constant J^2_{PP} values being around

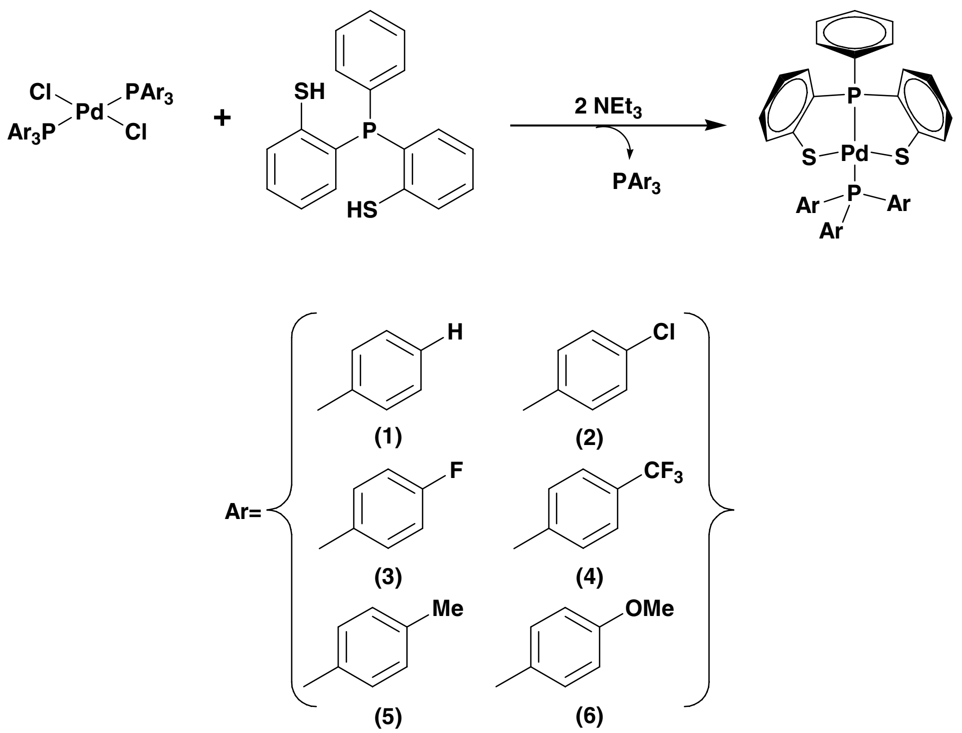

Scheme 1. Synthesis of $[Pd(\textit{ph}PS_2)(PAr_3)]$ Ar = C_6H_5 (**1**), C_6H_4-4-Cl (**2**), C_6H_4-4-F (**3**), C_6H_4-4-CF_3 (**4**), C_6H_4-4-Me (**5**), C_6H_4-4-OMe (**6**) complexes.

405 Hz, respectively (see Section 2). These values are also in agreement with a *trans* conformation for the two phosphorus nuclei in all cases [14]. The $^{31}P\{^1H\}$ results are very diagnostic of the identity of the complexes, while the observed variations in the chemical shift of the signals is a clear indicative of the electronic effect of the different *para*-substituents at the triarylphosphines. For instance, for complexes $[Pd(\textit{ph}PS_2)\{P(C_6H_4\text{-}4\text{-}CF_3)_3\}]$ (**4**) and $[Pd(\textit{ph}PS_2)\{P(C_6H_4\text{-}4\text{-}OMe)_3\}]$ (**6**) the phosphorus signals for $\textit{ph}PS_2{}^{-2}$ appear at $\delta = 86.78$ and 84.59 ppm, respectively; these two examples representing the upper and lower limits in the series of complexes. The results obtained can be rationalized in terms of the higher electron-withdrawing capability of –CF_3 with respect to that of the –OMe substituent, being higher in the case of complex **4** having the dishielding of the P nuclei in the S–P–S moiety as the ultimate consequence. Thus, the trend observed for the $^{31}P\{^1H\}$ $\textit{ph}PS_2{}^{-2}$ chemical shifts in the series of complexes $[Pd(\textit{ph}PS_2)(PAr_3)]$ goes: $[Pd(\textit{ph}PS_2)\{P(C_6H_4\text{-}4\text{-}OMe)_3\}]$ (**6**) (84.59 ppm) < $[Pd(\textit{ph}PS_2)\{P(C_6H_4\text{-}4\text{-}Me)_3\}]$ (**5**) (84.89 ppm) < $[Pd(\textit{ph}PS_2)(PPh_3)]$ (**1**) (85.33 ppm) < $[Pd(\textit{ph}PS_2)\{P(C_6H_4\text{-}4\text{-}F)_3\}]$ (**3**) (85.74 ppm) < $[Pd(\textit{ph}PS_2)\{P(C_6H_4\text{-}4\text{-}Cl)_3\}]$ (**2**) (86.04 ppm) < $[Pd(\textit{ph}PS_2)\{P(C_6H_4\text{-}4\text{-}CF_3)_3\}]$ (**4**) (86.78 ppm). This linear trend can be better observed in the following graphic where the chemical shift values are plotted versus the Hammet parameter for the phosphines employed (Graphic 1).

As expected from the structural similarity of the complexes, analysis by FAB^+–MS shows in all cases the molecular ion with the appropriate isotope distribution [15]. Another major common peak due to the loss of the corresponding ligand PAr_3 is also observed in all cases. For all complexes, elemental analysis are in good agreement with the proposed formulations.

The crystals suitable for single crystal X-ray diffraction analysis were obtained for complexes $[Pd(\textit{ph}PS_2)(PPh_3)]$ (**1**) [10], $[Pd(\textit{ph}PS_2)\{P(C_6H_4\text{-}4\text{-}Cl)_3\}]$ (**2**), $[Pd(\textit{ph}PS_2)\{P(C_6H_4\text{-}4\text{-}F)_3\}]$ (**3**), $[Pd(\textit{ph}PS_2)\{P(C_6H_4\text{-}4\text{-}Me)_3\}]$ (**5**) and $[Pd(\textit{ph}PS_2)\{P(C_6H_4\text{-}4\text{-}OMe)_3\}]$ (**6**). Several attempts to obtain suitable crystals of complex **4** were unfruitful. As expected, these structures share a number of common structural features, showing in all cases the palladium centers to be into slightly distorted square planar environments. The coordination sphere for all complexes being constituted for the ligand $\textit{ph}PS_2{}^{-2}$ coordinated in a tridentate S–P–S pincer like fashion and completed by the *p*-substituted triarylphosphine (PAr_3) located *trans* to the phosphorus atom of the ligand $\textit{ph}PS_2{}^{-2}$. The main distortion from the square planar geometry is caused in all cases by the rigidity of the $\textit{ph}PS_2{}^{-2}$ ligand and reflected in the angles S(1)–Pd(1)–S(2) and in a less pronounced manner in the vector P(1)–Pd(1)–P(2) (Table 2). The Pd–P(2) distances are slightly longer in the complexes having phosphines with electron-donating groups [–OMe (**6**) 2.3660(13) Å, –Me (**5**) 2.3690(14) Å] in comparison with those observed in the complexes bearing PAr_3 with electron-withdrawing groups [–Cl (**2**) 2.3443(15) Å, –F (**3**) 2.3598(9) Å] (Table 2), this, due in part to the more pronounced π-backbonding effect of the latter groups. The

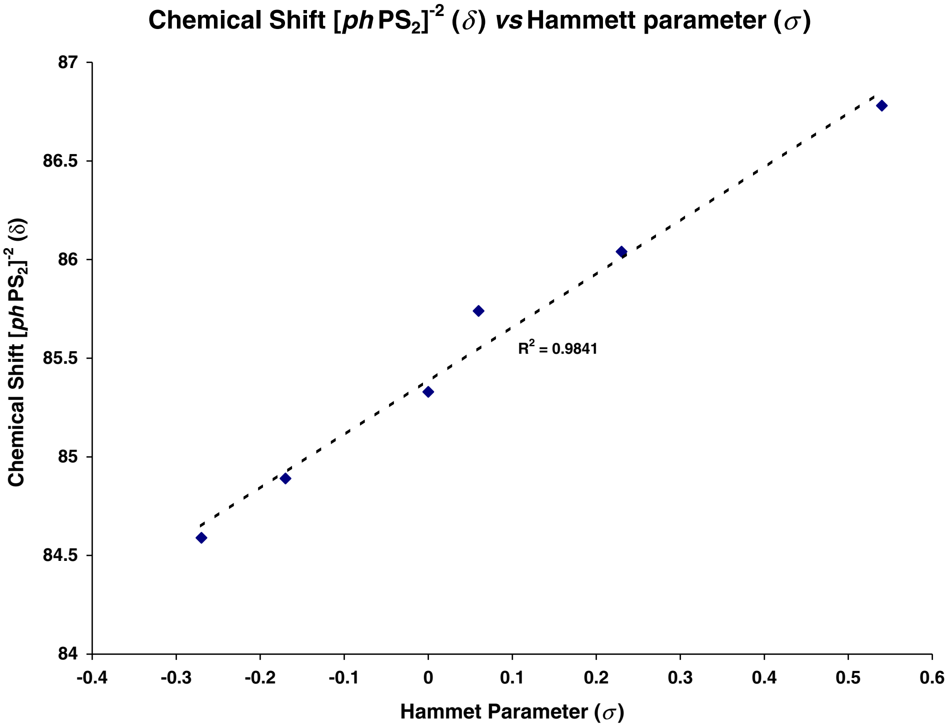

Graphic 1.

Pd–S distances are slightly different and comparable to those found in other palladium complexes (Table 2).

The determination of the melting point of the different [Pd(*ph*PS$_2$)(PAr$_3$)] compounds suggest these complexes to have a considerable stability to high temperatures, exhibiting melting points within the range of 200 and 240 °C without any visible decomposition. Based on these observations and the fact that the *ph*PS$_2$$^{-2}$ ligand may indeed behave as a hemilabile ligand thus promoting the reactivity of these complexes [16], we decided to examine the catalytic activity of these species in the olefination of halobenzenes (Heck reaction) by studying the C–C couplings between styrene and iodo or bromobenzene (Scheme 2). The stability of these SPS-Pd pincer complexes to air and moisture allowed us to carry out the catalytic reactions in a completely aerobical environment using reagent grade substrates. Initial screening of the reactions of styrene (3.2 mmol) with iodo or bromobenzene (2.5 mmol) using complex **1** as catalyst (4.33×10^{-3} mmol) in *N*,*N*′-dimethylformamide (DMF) (3 mL) and Na$_2$CO$_3$ (3.77 mmol) as the base afforded in both cases quantitative yields after 24 h reaction at 160 °C. The initial choice of Na$_2$CO$_3$ is due to the fact that it is a solid in the reaction mixture that remains in the solid state having the sole effect of scavenging the acid formed during the reaction without any further interference in the catalytic process. Furthermore, from the economical point of view this compound results the cheapest from a series of potential bases employed to date for this process. However, further experiments reducing the reaction time to only 4 hours, to better observe the effect of the base, revealed that it is in fact Cs$_2$CO$_3$ with a 76% conversion to stilbenes, a far better base than Na$_2$CO$_3$ with only 38% conversion and Et$_3$N with a 43% conversion under the same reaction conditions. With these results in hand and under these optimized reaction conditions we proceeded to determine which compound of the series was the best catalyst for the coupling of styrene and bromobenzene. The results obtained revealed that it is in fact complex [Pd(*ph*PS$_2$)(PPh$_3$)] (**1**) the more active catalyst precursor (Table 3). However, from the results shown in Table 3 it seems that apparently the *para*-substituted phosphines have little or no effect in the process. These results lead

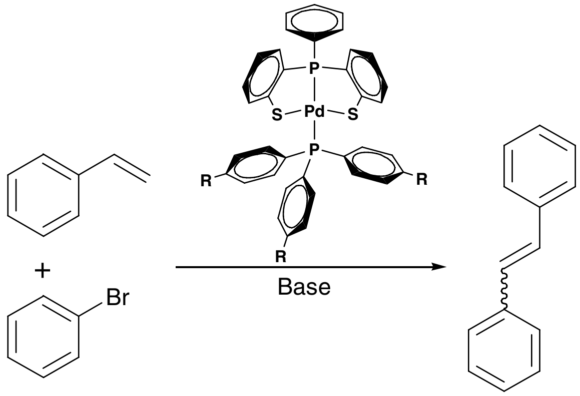

Scheme 2. Heck reaction using [Pd(*ph*PS$_2$)(PAr$_3$)] Ar = C$_6$H$_5$ (**1**), C$_6$H$_4$-4-Cl (**2**), C$_6$H$_4$-4-F (**3**), C$_6$H$_4$-4-CF$_3$ (**4**), C$_6$H$_4$-4-Me (**5**), C$_6$H$_4$-4-OMe (**6**) complexes as catalysts.

Table 3
Heck couplings of bromobenzene with styrene using [Pd(*ph*PS_2)(PAr_3)] Ar = C_6H_5 (**1**), C_6H_4-4-Cl (**2**), C_6H_4-4-F (**3**), C_6H_4-4-CF_3 (**4**), C_6H_4-4-Me (**5**), C_6H_4-4-OMe (**6**) as catalysts

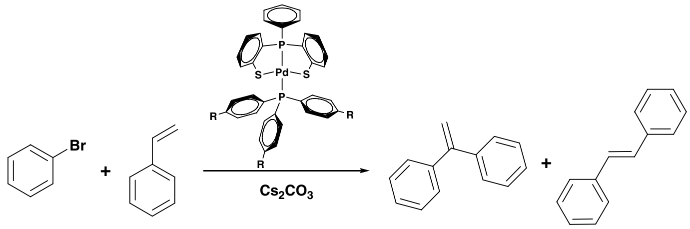

PAr_3	Hammett parameter	*gem*-Stilbene	*trans*-Stilbene	Conversion[a] (%)
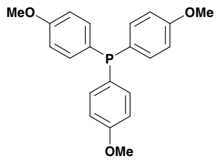	−0.27	9.83	64.22	74.05
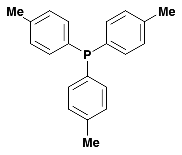	−0.17	9.41	60.59	70.00
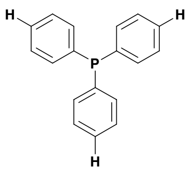	0.00	10.62	65.53	76.15
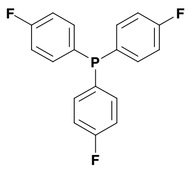	0.06	8.25	57.24	65.49
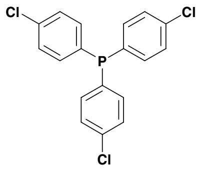	0.23	10.82	64.14	74.96
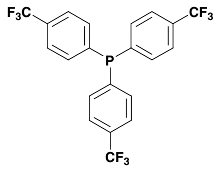	0.54	9.40	61.30	70.70

Reaction conditions: 2.5 mmol of halobenzene, 3.2 mmol of styrene, 3.77 mmol of base Cs_2CO_3, 4.33×10^{-3} mmol of catalyst and 3 ml of DMF, 4 h at 160 °C.
[a] Yields obtained by GC are based on bromobenzene and the average of two runs.

us to conclude that probably the initial step for the reaction mechanism using these complexes may involve the de-ligation of the phosphine PAr_3 to generate the necessary coordination site for the incoming substrates, which will later be reduced to allow the oxidative addition of the halogenated substrate over the Pd center.

Table 4
Heck couplings of *p*-substituted bromobenzenes with styrene using [Pd(*ph*PS$_2$)(PPh$_3$)] (**1**) as catalyst

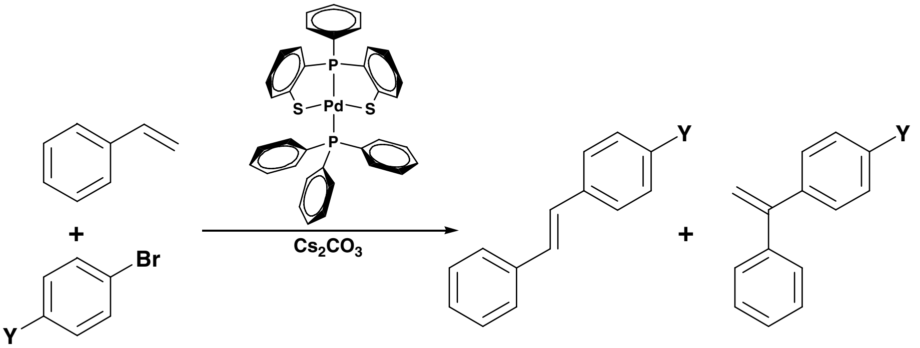

Ar–Br	Hammett parameter (σ)	*gem*-Stilbene	*trans*-Stilbene	Conversion[a] (%)
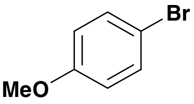	−0.27	2.55	29.94	32.49
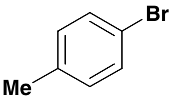	−0.17	2.62	33.88	36.50
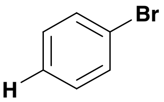	0	7.66	65.53	76.15
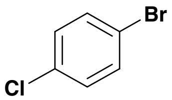	0.23	1.74	46.31	49.86
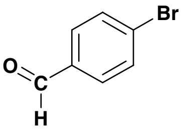	0.42	6.05	84.54	100.0

Reaction conditions: 2.5 mmol of halobenzene, 3.2 mmol of styrene, 3.77 mmol of base Cs$_2$CO$_3$, 4.33×10^{-3} mmol of catalyst and 3 ml of DMF, 4 h at 160 °C.

[a] Yields obtained by GC are based on halobenzene and the average of two runs.

Additionally, we decide to explore further the reactivity of complex [Pd(*ph*PS$_2$)(PPh$_3$)] (**1**) against a series of *para*-substituted bromobenzenes, the results obtained from these experiments show that electron-withdrawing groups in the aromatic ring of the bromobenzenes favor the Pd catalytic coupling with styrene, having conversions of up to 99% for *p*-bromobenzaldehyde, these results can be rationalized in terms of inductive effects, that in the case of bromobenzenes bearing electron-donating groups, the excess of electronic density would ultimately strengthen the C–Br bond thus making its activation more difficult. The reverse effect can be considered in the case of *p*-bromobenzenes having electron-withdrawing substituents (Table 4), although it is not clear why the point corresponding to bromobenzene lays out of the trend. Experiments aimed to clear this point are currently under investigation in our research group.

Experiments using chlorobenzene resulted only in traces of the products probably as a consequence of the quick and clear decomposition of the complexes in the reaction mixture to palladium black.

There has been a considerable debate in the literature about the oxidation states of the species involved in the catalytic cycle with Pd(IV)/Pd(II) and Pd(II)/Pd(0), both being proposed at various times [3,17], however, in this case given the type of species involved we favor the Pd(0)/Pd(II) mechanism although the precise mechanism of the catalytic reaction remains to be elucidated.

In summary, we have reported a series of complexes of the type [Pd(*ph*PS$_2$)(PAr$_3$)]. These compounds have been evaluated in the palladium catalyzed Heck reaction of iodo, bromo and chlorobenzene with styrene. Preliminary catalytic experiments indicate these complexes to be efficient catalyst in the Heck reaction. Analysis of the electronic effects of the *para*-substituted triarylphosphines on the performance of the different complexes reveal that these ligands are easily displaced from the coordination sphere of the complexes and have little or no effect in the performance of the catalytic precursor, thus it is fair to conclude that the series of [Pd(*ph*PS$_2$)(PAr$_3$)] complexes catalyze the Heck couplings of styrene and halobenzenes by a common intermediate. Efforts aimed to employ these compounds in other metal mediated organic syntheses and other cross-coupling reactions are currently under investigation.

4. Supplementary material

CCDC 612748, 612749, 612750 and 612751 contain the supplementary crystallographic data for **2**, **3**, **5** and **6**. The data can be obtained free of charge via htpp://www.ccdc.cam.ac.uk/conts/retrieving.html, or from the Cambridge Crystallographic Data Centre, 12 Union Road, Cambridge CB2 1EZ, UK; fax: (+44) 1223-336-033; or e-mail: deposit@ccdc.cam.ac.uk.

Acknowledgements

V.G.-B. would like to thank CONACYT, DGEP and DGAPA for financial support. We would like to thank Chem. Eng. Luis Velasco Ibarra and M.Sc. Francisco Javier Perez Flores for their invaluable help in the running of the FAB-Mass Spectra. The support of this research by CONACYT (J41206-Q) and DGAPA-UNAM (IN114605) is gratefully acknowledged.

References

[1] B. Cornils, W.A. Herrmann (Eds.), Applied Homogeneous Catalysis with Organometallic Compounds, vol. 2, Wiley-VCH Verlag GmbH, Federal Republic of Germany, 2002 (Chapter 3).
[2] (a) A. de Meijere, F. Diederich (Eds.), Metal-Catalyzed Cross-Coupling Reactions, 2nd ed., Wiley-VCH Verlag GmbH, Federal Republic of Germany, 2004;
(b) N. Miyaura (Ed.), Topics In Current Chemistry. Cross-Coupling Reactions: A Practical Guide, vol. 219, Springer, 2002.
[3] I.P. Beletskaya, A.V. Cheprakov, Chem. Rev. 100 (2000) 3009.
[4] A.M. Rouhi, Chem. Eng. News 82 (2004) 49.
[5] (a) N. Wheatley, J.R. Dilworth, Coord. Chem. Rev. 199 (2000) 89;
(b) J.R. Dilworth, P. Arnold, D. Morales, Y.L. Wong, Y. Zheng, The Chemistry and Applications of Complexes with Sulphur Ligands, in: Modern Coordination Chemistry, The Legacy of Joseph Chatt, Cambridge, UK, 2002, p. 217;
(c) M. Hiraoka, A. Nishikawa, T. Morimoto, K. Achiwa, Chem. Pharm. Bull. 46 (1998) 704;
(d) E. Hauptman, R. Shapiro, W. Marshall, Organometallics 17 (1998) 4976;
(e) E. Hauptman, P.J. Fagan, W. Marshall, Organometallics 18 (1999) 2061;
(f) H-S. Lee, J-Y. Bae, J. Ko, Y.S. Kang, H.S. Kim, S.O. Kang, Chem. Lett. (2000) 602;
(g) A.S. Abu-Surrah, K. Lappalainen, T. Repo, M. Klinga, M. Leskelä, H.A. Hodali, Polyhedron 19 (2000) 1601;
(h) D.A. Evans, K.R. Campos, J.S. Tedrow, F.E. Michael, M.R. Gagné, J. Am. Chem. Soc. 122 (2000) 7905;
(i) J.R. Dilworth, D. Morales, Y. Zheng, J. Chem. Soc., Dalton Trans. (2000) 3007;
(j) D. Morales-Morales, S. Rodríguez-Morales, J.R. Dilworth, A. Sousa-Pedrares, Y. Zheng, Inorg. Chim. Acta 332 (2002) 101;
(k) D. Canseco-González, V. Gómez-Benítez, S. Hernández-Ortega, R.A. Toscano, D. Morales-Morales, J. Organomet. Chem. 679 (2003) 101;
(l) D. Canseco-González, V. Gómez-Benítez, O. Baldovino-Pantaleón, S. Hernández-Ortega, D. Morales-Morales, J. Organomet. Chem. 689 (2004) 174;
(m) G. Ríos-Moreno, R.A. Toscano, R. Redón, H. Nakano, Y. Okuyama, D. Morales-Morales, Inorg. Chim. Acta. 358 (2005) 303.
[6] (a) C.S. Stone, D.D. Weinberger, C.A. Mirkin, Prog. Inorg. Chem. 48 (1999) 233;
(b) P. Braunstein, F. Naud, Angew. Chem., Int. Ed. Engl. 40 (2001) 680.
[7] (a) D. Morales-Morales, C. Grause, K. Kasaoka, R. Redón, R.E. Cramer, C.M. Jensen, Inorg. Chim. Acta 300–302 (2000) 958;
(b) D. Morales-Morales, R. Redón, Z. Wang, D.W. Lee, C. Yung, K. Magnuson, C.M. Jensen, Can. J. Chem. 79 (2001) 823;
(c) D. Morales-Morales, R. Redón, D.W. Lee, Z. Wang, C.M. Jensen, Organometallics 20 (2001) 1144;
(d) D. Morales-Morales, R.E. Cramer, C.M. Jensen, J. Organomet. Chem. 654 (2002) 44;
(e) X. Gu, W. Chen, D. Morales-Morales, C.M. Jensen, J. Mol. Catal. A. 189 (2002) 119;
(f) D. Morales-Morales, R. Redón, C. Yung, C.M. Jensen, Inorg. Chim. Acta 357 (2004) 2953;
(g) O. Baldovino-Pantaleón, S. Hernández-Ortega, D. Morales-Morales, Inorg. Chem. Commun. 8 (2005) 955;
(h) O. Baldovino-Pantaleón, S. Hernández-Ortega, D. Morales-Morales, Adv. Synth. Catal. 348 (2006) 236;
(i) F.E. Hahn, M.C. Jahnke, V. Gómez-Benítez, D. Morales-Morales, T. Pape, Organometallics 24 (2005) 6458;
(j) Z. Wang, S. Sugiarti, C.M. Morales, C.M. Jensen, D. Morales-Morales, Inorg. Chim. Acta 359 (2006) 1923;
(k) V. Gómez-Benítez, O. Baldovino-Pantaleón, C. Herrera-Álvarez, R.A. Toscano, D. Morales-Morales, Tetrahedron Lett. 47 (2006) 5059;
(l) O. Baldovino-Pantaleón, J. Barroso-Flores, J.A. Cogordan, S. Hernández-Ortega, R.A. Toscano, D. Morales-Morales, J. Mol. Catal. A. Chem. 247 (2006) 65;
(m) R. Cerón-Camacho, V. Gómez-Benítez, R. Le Lagadec, D. Morales-Morales, R.A. Toscano, J. Mol. Catal. A. Chem. 247 (2006) 124.
[8] E. Bloch, V. Eswarakrishnan, M. Gernon, G. Ofori-Okai, C. Saha, K. Tang, J. Zubieta, J. Am. Chem. Soc. 111 (1989) 658.
[9] J. Chatt, F.G. Mann, J. Chem. Soc. (1939) 1622.
[10] V. Gómez-Benítez, S. Hernández-Ortega, D. Morales-Morales, Inorg. Chim. Acta 346 (2003) 256.
[11] G.M. Sheldrick, Acta Crystallogr. Sect. A. 46 (1990) 467.

[12] G.M. Sheldrick, SHELXL-97, Program for Crystal Structure Refinement, University of Göttingen, 1998.

[13] L.J. Farrugia, ORTEP-3 for Windows. J. Appl. Crystallogr. 30 (1997) 565.

[14] L.D. Quin, J.G. Verkade, Phosphorus-31 NMR Spectral Properties in Compound Characterization and Structural Analysis, John Wiley & Sons, Inc., 1994.

[15] J.J. Manura, D.J. Manura, Isotope Distribution Calculator, Scientific Instrument Service, 1996.

[16] V. Gómez-Benítez, R.A. Toscano, D. Morales-Morales, Inorg. Chem. Commun. 10 (2007) 1.

[17] D. Morales-Morales, R. Redón, C. Yung, C.M. Jensen, Chem. Commun. (2000) 1619.